# MOR1, the *Arabidopsis thaliana* homologue of *Xenopus* MAP215, promotes rapid growth and shrinkage, and suppresses the pausing of microtubules in vivo

**Eiko Kawamura and Geoffrey O. Wasteneys***

Department of Botany, University of British Columbia, Vancouver, BC, Canada V6T 1Z4

*Author for correspondence (e-mail: geoffwas@interchange.ubc.ca)

*Accepted 9 September 2008*
*Journal of Cell Science 121, 4114-4123 Published by The Company of Biologists 2008*
*doi:10.1242/jcs.039065*

## Summary

**MOR1, the *Arabidopsis thaliana* homologue of the *Xenopus* microtubule-associated protein MAP215, is required for spatial organization of the acentrosomal microtubule arrays of plant cells. To determine how loss of MOR1 function affects microtubule dynamics, we compared various parameters of microtubule dynamics in the temperature-sensitive *mor1-1* mutant at its permissive and restrictive temperatures, 21°C and 31°C, respectively. Dynamic events were tracked in live cells expressing either GFP-tagged β-tubulin or the plus end tracking EB1. Microtubule growth and shrinkage velocities were both dramatically reduced in *mor1-1* at 31°C and the incidence and duration of pause events increased. Interestingly, the association of EB1 with microtubule plus ends was reduced in *mor1-1* whereas side wall binding increased, suggesting that MOR1 influences the association of EB1 with microtubules either by modulating microtubule plus end structure or by interacting with EB1. Although *mor1-1* microtubules grew and shrank more slowly than wild-type microtubules at 21°C, the incidence of pause was not altered, suggesting that pause events, which occur more frequently at 31°C, have a major detrimental role in the spatial organization of cortical microtubules. Extensive increases in microtubule dynamics in wild-type cells when shifted from 21°C to 31°C underline the importance of careful temperature control in live cell imaging.**

Supplementary material available online at
http://jcs.biologists.org/cgi/content/full/121/24/4114/DC1

Key words: Microtubule dynamics, Microtubule-associated protein, TOG domain, HEAT repeat, *Arabidopsis thaliana*, Acentrosomal microtubules

## Introduction

Microtubules are highly dynamic structures that undergo transitions between states of growth, shrinkage and pause. In vitro experiments demonstrate that these transitions rely on the hydrolysis of GTP bound to the exposed β-tubulin moiety, with the growing ends of microtubules protected from catastrophe when polymerization rates exceed GTP hydrolysis. Conversely, depolymerization is encouraged when GDP-bound subunits are exposed. This model for microtubule dynamics is insufficient for the living cell, in which the complex dynamic properties of microtubules are regulated by the activity of microtubule-associated proteins.

The MAP215 proteins [CKAP5 (or TOGp) in human, Msps in *Drosophila*, ZYG-9 in *C. elegans*, Stu2 in *S. cerevisiae*, Dis1 or Alp14 in *S. pombe*, CP224 in *Dictyostelium*, MOR1 in *Arabidopsis*] are perhaps the most ubiquitous and conserved of microtubule-associated proteins. They are found in eukaryotic organisms from all kingdoms and appear to be essential for survival (Gard et al., 2004). The exact mechanism by which they regulate microtubule dynamics is gradually becoming clearer (Brouhard et al., 2008) yet there are several contradictory claims regarding their function in regulating microtubule dynamics (Popov and Karsenti, 2003). MAP215 was first identified in *Xenopus* egg cytoplasmic extracts as a factor promoting the elongation and stability of microtubules (Gard and Kirchner, 1987) but a later screen isolated XMAP215 as a major microtubule-destabilizing factor (Shirasu-Hiza et al., 2003). There is similar uncertainty about the role of the budding yeast orthologue Stu2 in microtubule dynamics. In vivo depletion of Stu2 can induce less dynamic cytoplasmic microtubules, with suppression of rescue and catastrophe and increased pausing time (Kosco et al., 2001). In vitro analysis, however, indicates that Stu2 acts primarily to destabilize microtubules (van Breugel et al., 2003).

The contrasting functions of XMAP215 homologues in microtubule dynamics are partly resolved by in vitro studies that have demonstrated that XMAP215 is able to promote both growth and shrinkage of microtubules. The earliest of these studies determined by video-enhanced microscopy that in the presence of 0.2 μM XMAP215, microtubules nucleating from axoneme fragments showed a seven- to tenfold increase in elongation velocity, a threefold increase in shortening velocity, and near-elimination of rescue events (Vasquez et al., 1994). Later, when optical tweezers were used to measure with great precision the velocity of microtubule growth and shrinkage from axonemes (Kerssemakers et al., 2006), the addition of XMAP215 not only increased growth and shrinkage velocities but appeared to generate incremental growth spurts of 40-60 nm, suggesting the addition of oligomers of tubulin. Most recently, total internal reflection fluorescence microscopy was used to measure up to tenfold increases in both microtubule growth and shrinkage velocities in the presence of XMAP215, suggesting that depolymerization is simply a reversal of the growth reaction catalyzed by XMAP215

(Brouhard et al., 2008). The cellular environment is vastly more complex than the contents of a test tube, so any attribute identified through in vitro observation should be validated in a cellular environment. This is especially pertinent to the XMAP215 family of proteins, whose effectiveness in regulating microtubule dynamics varies according to the activities of mitotic CDK (Vasquez et al., 1999), EB1 and catastrophe-promoting kinesins (Cassimeris and Morabito, 2004; Kinoshita et al., 2001; Tournebize et al., 2000), and the degree of interaction with these and other members of an extensive protein network (Niethammer et al., 2007).

In vivo analysis of knock-out alleles is not feasible on account of the essential nature of XMAP215 family proteins, which renders null alleles lethal. Depleting the protein through knock-down approaches (Brittle and Ohkura, 2005; Kosco et al., 2001) is promising but some fully functional protein is likely to remain, limiting the conclusions that can be drawn. Alternatively, mutant alleles that alter the functional properties of the protein without altering expression can be used. The *mor1-1* and *mor1-2* alleles of the *Arabidopsis thaliana* XMAP215 homologue MOR1 (Whittington et al., 2001) provide an excellent in vivo model system to explore the function of XMAP215 proteins. In the *mor1-1* mutant, cortical microtubule arrays (Whittington et al., 2001), as well as mitotic and cytokinetic arrays (Kawamura et al., 2006) undergo rapid changes to become disrupted at temperatures above 28°C. Analysis of microtubule organization in fixed or living cells of the *mor1-1* mutant, however, has so far been restricted to analysis of array organization (Kawamura et al., 2006) and no detailed analysis of single microtubule dynamics has been attempted. It has been shown that microtubules are short and disordered spatially at restrictive temperature (Kawamura et al., 2006) and that plant growth is hypersensitive to microtubule destabilizing drugs (Collings et al., 2006). In vitro analysis of the MOR1 tobacco homologue MAP200 suggests that it increases the number and length of microtubules (Hamada et al., 2004). Taken together, these reports support the role of MOR1 in promoting microtubule growth but provide no evidence for its promotion of microtubule disassembly.

In this study, we employed spinning disc confocal microscopy to quantify the specific effects of the *mor1-1* mutation on microtubule dynamics in vivo. We show that the *mor1-1* mutation dramatically reduces both microtubule growth and shrinkage rates at the 31°C restrictive temperature and that it increases the proportion of time spent in pause at the expense of growth.

## Results

We sought to quantify the effects of the *mor1-1* temperature-sensitive mutation on several parameters of microtubule dynamics using GFP reporter proteins in living epidermal cells of the first leaf. After testing several available fluorescent reporters, we chose to use the GFP–β-tubulin reporter line, *Pro35S*::GFP-TUB (Nakamura et al., 2004). This GFP-TUB line has relatively low fluorescence intensity but produces no detectable morphological phenotypes, as has been demonstrated for the MBD-GFP (Marc et al., 1998) and GFP-TUA (Ueda et al., 1999) reporters (Abe and Hashimoto, 2005; Wasteneys and Yang, 2004). To minimize phototoxicity and to capture sufficient fluorescent signal, we used spinning disc confocal microscopy, and recorded time-lapse series of several seconds to several minutes. A temperature-controlled stage and an objective heater kept the specimens at restrictive or permissive temperatures throughout imaging. Data from the *Pro35S*::GFP-TUA line, which were collected using a conventional confocal microscope, are provided in the supplementary material (supplementary material Fig. S1). At 31°C, only microtubules with both ends in focus were used for measurements so that we could distinguish and track the changes in both plus and minus ends. Microtubule minus ends were very static, spending over 95% of the time in pause in *mor1-1* and wild-type cells at both 21°C and 31°C (supplementary material Fig. S2). Growth events at the minus ends were exceedingly rare and short-lived. Shrinkage events at microtubule minus ends were observed more frequently but, although shrinkage velocity (generally around 2 μm/minute) could sometimes be measured, the sample size was insufficient to draw any meaningful comparison between genotypes and temperatures. This article therefore reports on microtubule plus end dynamics.

### High temperature accelerates microtubule growth and shrinkage in wild-type cells

Before measuring the effect of the *mor1-1* mutation on plus end microtubule dynamics, we first assessed wild-type microtubule dynamics at the permissive and restrictive temperatures of *mor1-1* of 21°C and 31°C, respectively (Fig. 1A,B). At 21°C, a mean growth speed of 3.5±1.9 μm/minute and a mean shrinkage speed of –9.0±5.8 μm/minute was calculated (Fig. 1A, Fig. 2, Fig. 3A; supplementary material Movie 1). At 31°C, speeds increased significantly to 6.5±3.5 μm/minute ($P<1.0^{-16}$) for growth and –12.4±9.3 μm/minute ($P=0.013$) for shrinkage (Fig. 1B, Fig. 2, Fig. 3B; supplementary material Movie 2). This indicates that moderate temperature increases stimulate high microtubule growth and shrinkage rates in wild-type cells, and that future studies on microtubule dynamics in plant cells need to monitor and record temperature using appropriate temperature control devices.

### Microtubule dynamics are reduced in the *mor1-1* mutant even at the permissive temperature

Microtubule plus end dynamics were next compared in wild type and *mor1-1* at the permissive temperature, 21°C. In agreement with previous studies using immunofluorescence or other GFP reporters (Sugimoto et al., 2003; Whittington et al., 2001), cortical microtubule organization visualized with GFP-TUB appeared normal in *mor1-1* (Fig. 1C). Nevertheless, we found that microtubule dynamics were in fact slightly but significantly different. In *mor1-1*, both microtubule growth (*mor1-1*: 2.5±1.5 μm/minute; wild type: 3.5±1.9 μm/minute) and shrinkage rates (*mor1-1*: –6.2±4.3 μm/minute; wild type: –9.0±5.8 μm/minute) were significantly reduced compared with the wild type ($P<1.0^{-13}$ and $P<1.0^{-3}$, respectively; Fig. 2, Fig. 3A,C; compare also Movies 1 and 3 in supplementary material). These results show that the *mor1-1* mutation affects microtubule dynamics even at the permissive temperature, though it would appear that these changes in microtubule polymerization and depolymerization dynamics are not sufficient to introduce detectable changes in the spatial organization of microtubule arrays or measurable growth anomalies.

### Microtubule growth and shrinkage rates are decreased in the *mor1-1* mutant at restrictive temperature

From time-lapse images of GFP-TUB, the *mor1-1* microtubule plus ends became strikingly less dynamic at 31°C. As shown in Fig. 1D and supplementary material Movie 4, some microtubule ends in *mor1-1* were so static that plus ends displayed dynamics similar to that normally found at minus ends. Kymographs of microtubules

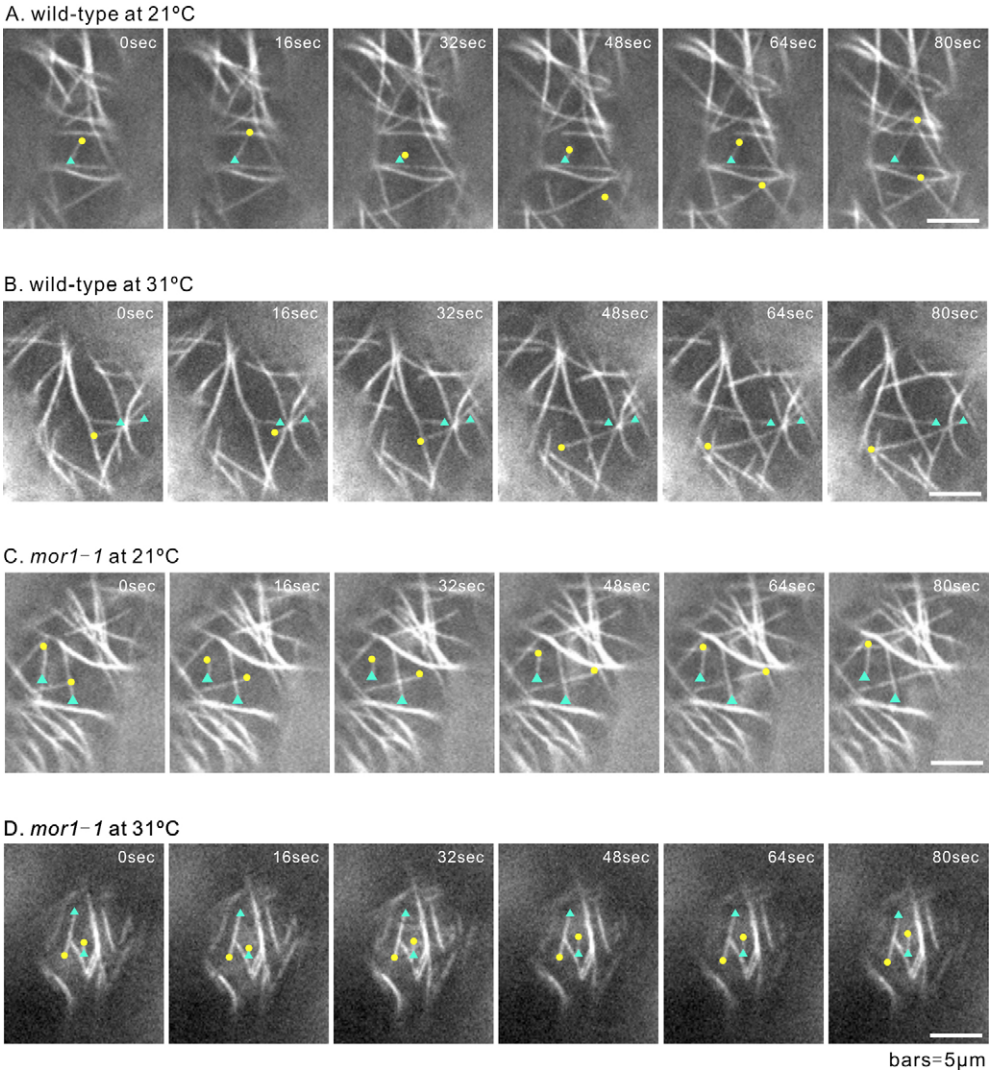


**Fig. 1.** Comparison of microtubule dynamics in the *mor1-1* mutant and the wild type. (A) Wild type at 21°C (corresponds to Movie 1 in supplementary material); (B) wild type at 31°C (corresponds with Movie 2 in the supplementary material); (C) *mor1-1* at 21°C (corresponds to Movie 3 in supplementary material); (D) *mor1-1* at 31°C (corresponds with Movie 4 in supplementary material). Representative time-lapse series of microtubules labelled by expression of the 35S driven GFP-TUB reporter are shown, as collected from epidermal cells on the abaxial surface of first leaves from 11- to 12-day-old seedlings. Microtubule plus ends are indicated with yellow dots and minus ends are labelled with blue triangles. Time between frames was 8 seconds (see supplementary material Movies 1-4 ) but 16 second intervals are shown here. Images were collected with a spinning disc confocal microscope equipped with a temperature-controlled stage to keep specimens at 21°C or 31°C. Bars, 5 μm.

showed that velocity slopes in *mor1-1* were gentle whereas in wild type they were steep (Fig. 2). In *mor1-1*, average microtubule growth rates (*mor1-1*: 2.0±1.5 μm/minute; wild type: 6.5±3.5 μm/minute) and shrinkage rates (*mor1-1*: –3.8±3.1 μm/minute; wild type: –12.4±9.3 μm/minute) were significantly reduced compared to the wild type ($P<1.0^{-30}$ and $P<1.0^{-5}$, respectively; Fig. 3B,D). Although microtubules in wild-type cells became more dynamic with the temperature increase, microtubules in *mor1-1* cells at the restrictive temperature (Fig. 3B,D) grew ($P<1.0^{-4}$) and shrank ($P<1.0^{-5}$) more slowly than at the permissive temperature (Fig. 3A,C). In the *mor1-1* mutant, the GFP-TUB cytoplasmic fluorescence was greatly increased in comparison with wild type when similar contrast adjustments were applied (data not shown), indicating that a significant amount of GFP-TUB was unpolymerized. This is consistent with a previous report from hypocotyl cells using a GFP-TUA reporter (Whittington et al., 2001). In Fig. 1D the increased cytoplasmic fluorescence is not obvious because contrast was adjusted to reduce higher background fluorescence in *mor1-1*. Similar experiments using the GFP-TUA reporter and a conventional confocal microscope revealed similar trends (supplementary material Fig. S1). These data indicate that MOR1 normally promotes both rapid growth and shrinkage of microtubules.

### The *mor1-1* mutation alters the association of EB1 with microtubules

EB1 strongly associates with the growing plus ends of microtubules so that when fused to GFP, its fluorescence appears comet-like in time-lapse microscopy, which enables measurement of microtubule plus end behaviour (Bisgrove et al., 2004). To track EB1 comets we used the *ProEB1*::EB1b-GFP line (Dixit et al., 2006), which uses the endogenous promoter of the *Arabidopsis EB1b* gene to drive expression of EB1b tagged at its C terminus with GFP. Expression levels are lower than in lines in which GFP-EB1 expression is controlled by the 35S promoter. In *mor1-1* at the restrictive temperature, EB1 comets in the *ProEB1*::EB1b-GFP line were less abundant, smaller , had weaker fluorescence and were irregularly shaped when compared to the wild-type control line expressing the same construct (Fig. 4A, Fig. 5; supplementary material Movies 5-8). Background fluorescence was also increased (Fig. 5). EB1b-GFP comets in *mor1-1* cells were rarely observed for more than one or two time points (Fig. 4A, Fig. 5D; supplementary material Movie 8). Even when they were observed for longer periods of time, they remained in the same positions while comet size and intensity fluctuated (Fig. 4A) indicating the pausing of microtubules, or slower movement than in wild-type cells (Fig.

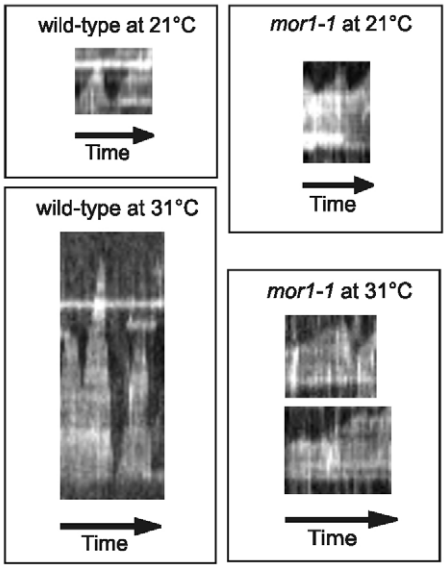


**Fig. 2.** Kymograph analysis of microtubule dynamics in wild type and *mor1-1*. Kymographs were created with ImageJ Multiple Kymograph using representative microtubules labelled with GFP-TUB in wild type and *mor1-1* at 21°C and 31°C, as described in Fig. 1. Two different kymographs are shown for *mor1-1* at the restrictive temperature (31°C).

4B). Close observation of comets demonstrated that EB1b-GFP labelling of *mor1-1* fluctuated from frame to frame even at the permissive temperature (Fig. 4A). These data confirm that MOR1 promotes constant growth of microtubules but also indicate that the microtubule plus end is unstable for EB1 association in the *mor1-1* mutant. As shown in Fig. 4B, the velocities of EB1b-GFP comets were consistent with the variable growth rates measured with GFP-TUB (Fig. 3) although in wild type (but not *mor1-1* cells) the growth rates were somewhat higher. The fastest movements of comets occurred in the wild type at 31°C (8.2±2.5 μm/minute) followed by wild type at 21°C (4.9±2.0 μm/minute), *mor1-1* at 21°C (2.3±1.5 μm/minute) and *mor1-1* at 31°C (1.4±1.3 μm/minute; Fig. 4B). These results also support the idea that MOR1 has a role in stabilizing growing microtubule plus ends, and demonstrate that higher temperature promotes faster microtubule polymerization in vivo.

Comparing the fluorescence intensity of EB1 comets suggested that the association of EB1 with microtubules fluctuates according to temperature but that there is no clear relationship with its affinity for plus ends and the speed of microtubule growth. In wild-type cells, in which EB1 comet velocities increased at 31°C, the average maximum fluorescence intensities of EB1 comets (shown in Fig. 4A, Fig. 6A,B) declined to 92% of the intensities measured in the same cells at 21°C, although according to the Wilcoxon signed-rank test this difference is not significant ($P>0.1$). In the *mor1-1* mutant at 31°C, microtubule growth rates were greatly reduced (Fig. 4B), and the average maximum fluorescence intensities of EB1b-GFP comets (shown in Fig. 6C,D) declined to 67% of the value measured at 21°C, which is a significant difference ($P<0.01$). The fact that wild-type EB1 comet intensity did not increase at faster growth rates demonstrates that the influence of MOR1 on EB1 plus end association is not merely through its modulation of plus end polymerization rate. Interestingly, microtubule side wall labelling by EB1b-GFP was frequently observed in *mor1-1* at 31°C (Fig. 6D).

## The *mor1-1* mutation increases the time microtubules spend in pause

To verify the observation that microtubules in *mor1-1* were relatively static at the restrictive temperature (Fig. 1D, Fig. 2; supplementary material Movie 4), we used data collected using the GFP-TUB reporter to calculate the percentage of overall time spent in each phase, including growth, shrinkage and pause (Fig. 7A,B). The proportion of time spent in each phase was very similar for wild type and *mor1-1* at 21°C (Fig. 7A) but at 31°C (Fig. 7B) microtubules in *mor1-1* cells spent about three times as long in pause as wild-type microtubules (*mor1-1*: 45%; wild type: 16%). The gain in time spent in pause in *mor1-1* came largely at the expense of time spent in growth, with the proportion of time spent in growth reduced by half in *mor1-1* (35%) compared with wild type (68%; Fig. 7B).

If microtubule plus ends tend to pause more frequently in *mor1-1*, it is possible that the initiation of pausing is promoted as well. Therefore we analyzed transition frequencies from growth or shrinkage to pause. As shown in Fig. 7C,D, the frequencies were both greatly increased in *mor1-1* at the restrictive temperature (*mor1-1*: 0.96 events/minute; wild type: 0.38 events/minute for growth to pause and *mor1-1*: 1.21 events/minute; wild type: 0.44 events/minute for shrinkage to pause). In a similar manner, if pause is promoted,

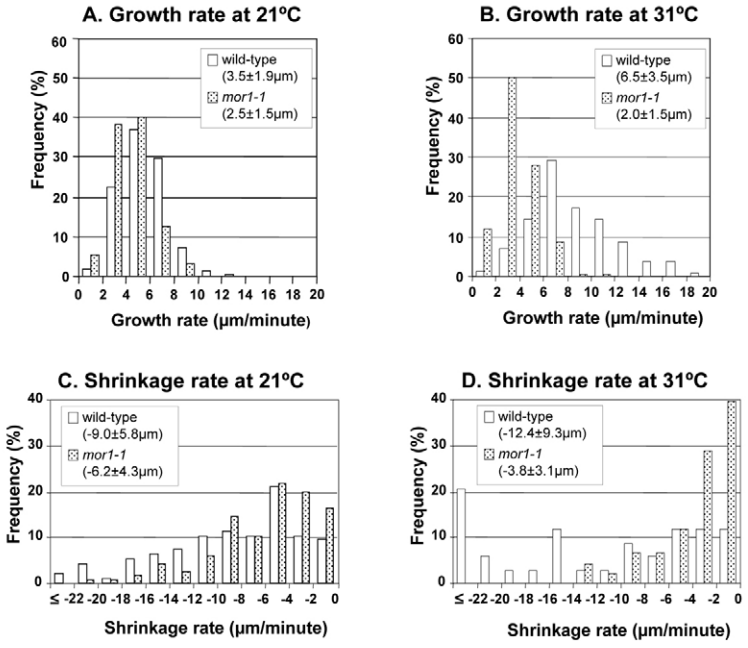


**Fig. 3.** Quantification of growth and shrinkage rates in wild type and *mor1-1* at 21°C and 31°C. Growth and shrinkage rates calculated from time-lapse images of microtubules expressing GFP-TUB as described in Fig. 1 are presented as frequency distribution histograms. Mean values are shown in the insets. (A) Growth rates at 21°C. (B) Growth rates at 31°C. (C) Shrinkage rates at 21°C. (D) Shrinkage rates at 31°C. Shrinkage rates greater than –22 μm/minute are shown as one data group (≤). Data were collected from 115 microtubules from six cells from four different plants for wild type at 21°C, 28 microtubules from seven cells from four different plants for wild type at 31°C, 98 microtubules from five cells from three different plants for *mor1-1* at 21°C, and 26 microtubules from 12 cells from nine different plants for *mor1-1* at 31°C.

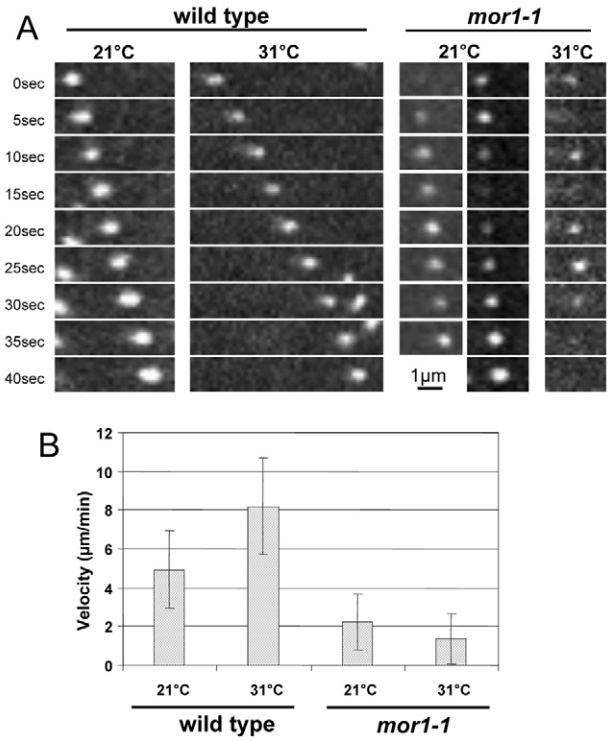


**Fig. 4.** EB1-GFP comet tracking of microtubule plus end dynamics in wild type and *mor1-1*. (A) Representative time-lapse images are displayed so that the relative velocities of EB1 comets are easily compared at 21°C and 31°C for wild type and *mor1-1*. Images were collected from the abaxial surface of first leaves of 11- to 12-day-old plants. The images of the wild type were obtained from single cells at both temperatures using identical confocal settings and digital processing. Contrast adjustments for the *mor1-1* images shown here varied, so the fluorescent intensities cannot be compared. (B) Quantification of *ProEB1*::EB1-GFP comet velocities in wild type and *mor1-1* at 21°C and 31°C. Data were generated from time-lapse images taken every 5 seconds, as shown in A. The velocities were measured from 296 comets from 18 cells from five different plants for wild type at 21°C, 126 comets from 12 cells from three different plants for wild type at 31°C, 157 comets from 10 cells from three different plants for *mor1-1* at 21°C and 142 comets from 12 cells from five different plants for *mor1-1* at 31°C. Bars indicate the standard deviation.

transition from pause to growth or shrinkage could be decreased so that microtubules would remain in pause phase. The frequency of transition from pause to growth was in fact decreased in *mor1-1* (*mor1-1*: 0.70 events/minute; wild type: 1.41 events/minute) yet frequency of transition from shrinkage to pause remained similar (*mor1-1*: 0.63 events/minute; wild type: 0.70 events/minute; Fig. 7C,D). These data indicate that growth events are suppressed in *mor1-1* whereas pause is promoted. Time spent in shrinkage, however, was similar in *mor1-1* (20%) and wild type (17%; Fig. 7B). At 21°C, there was not much difference in the time spent in each state between *mor1-1* and wild type (Fig. 7A). After the temperature increase, wild-type microtubules spent twice as much time in pause (21°C: 8%; 31°C: 16%) but the proportion of time spent growing and shrinking was only slightly reduced (Fig. 7B).

### Constant growth of microtubules is inhibited in the *mor1-1* mutant

Another general characteristic of microtubule dynamics in *mor1-1* at restrictive temperature was that microtubules appeared to be 'indecisive', spending relatively short periods of time in any given state before switching (Fig. 1; supplementary material Movie 4). In wild-type cells at 21°C, growth events consistently lasted for at least 24 seconds but at 31°C, shorter growth events lasting less than 16 seconds were detected. To quantify the duration of growth events, we calculated the proportion of microtubule ends that grew constantly for at least 8 seconds (the interval between two time frames), at least 16 seconds, and for more than 24 seconds (Fig. 8). In *mor1-1* at the restrictive temperature, the proportion of constant growth events that lasted 8 or 16 seconds was significantly greater than in wild type (*mor1-1*: 21%; wild type: 15% for 8 seconds, and *mor1-1*: 14%; wild type: 4% for 8-16 seconds). These findings were corroborated by the EB1 comet analysis (using 5-second intervals), which showed that in *mor1-1* at 31°C, many EB1b-GFP comets lasted for only 1 or 2 time points (Fig. 4).

## Discussion

By comparing several parameters of microtubule dynamics in the wild type and the *mor1-1* mutant, our study demonstrates that MOR1 promotes rapid growth and shrinkage while inhibiting pause events to keep microtubules highly dynamic. Importantly, these in vivo data corroborate recent in vitro experiments showing that the *Xenopus* homologue of MOR1, XMAP215, causes microtubules to both polymerize and depolymerize at greater velocities (Brouhard et al., 2008; Kerssemakers et al., 2006). Our results also provide important insights into the function of MOR1 in regulating the interactions of the microtubule plus end tracking protein EB1, and provide important baseline data on the influence of temperature on microtubule dynamics in plant cells.

### Possible mechanisms of microtubule dynamics regulation by MOR1

As a point mutant that generates aberrant function in a temperature-dependent manner, the *mor1-1* allele not only provides a useful measure for general function of MAP215 proteins but also provides insight into the specific functions of domains and subdomains of these MAPs. Severe as it is, the *mor1-1* phenotype does not constitute complete loss of function even at restrictive temperature. It is known, for example, that the mutant mor1-1 protein remains associated with microtubules at the restrictive temperature (Kawamura et al., 2006). This continued association with microtubule polymers is consistent with the fact that the phenylalanine substitution for leucine that causes the *mor1-1* phenotype is found in the N-terminal domain (Whittington et al., 2001), whereas microtubule binding appears to be conferred by motifs residing in the C-terminal 855 amino acids (Twell et al., 2002). The *mor1-1* mutation is located in an alpha helical stretch of the fifth HEAT-like repeat in the first of five N-terminal TOG domains, according to recent crystallography data (Al-Bassam et al., 2007; Slep and Vale, 2007). Interestingly, a nearly identical phenotype is caused by the glutamic acid to lysine substitution in the *mor1-2* allele in the opposing (return) alpha helix of the same HEAT-like repeat (Whittington et al., 2001). HEAT repeats are implicated in protein-protein interaction. The most probable candidate interactors with the HEAT-like repeats that make up the TOG domains of MAP215 family MAPs are α- and β-tubulins (Al-Bassam et al., 2007; Slep and Vale, 2007).

Live cell imaging data from the current study indicate that the N-terminal TOG domain, where the *mor1-1*, *mor1-2* (Whittington et al., 2001) and *rid5* (Konishi and Sugiyama, 2003) point mutations are all found, plays a key role in the tubulin polymerase

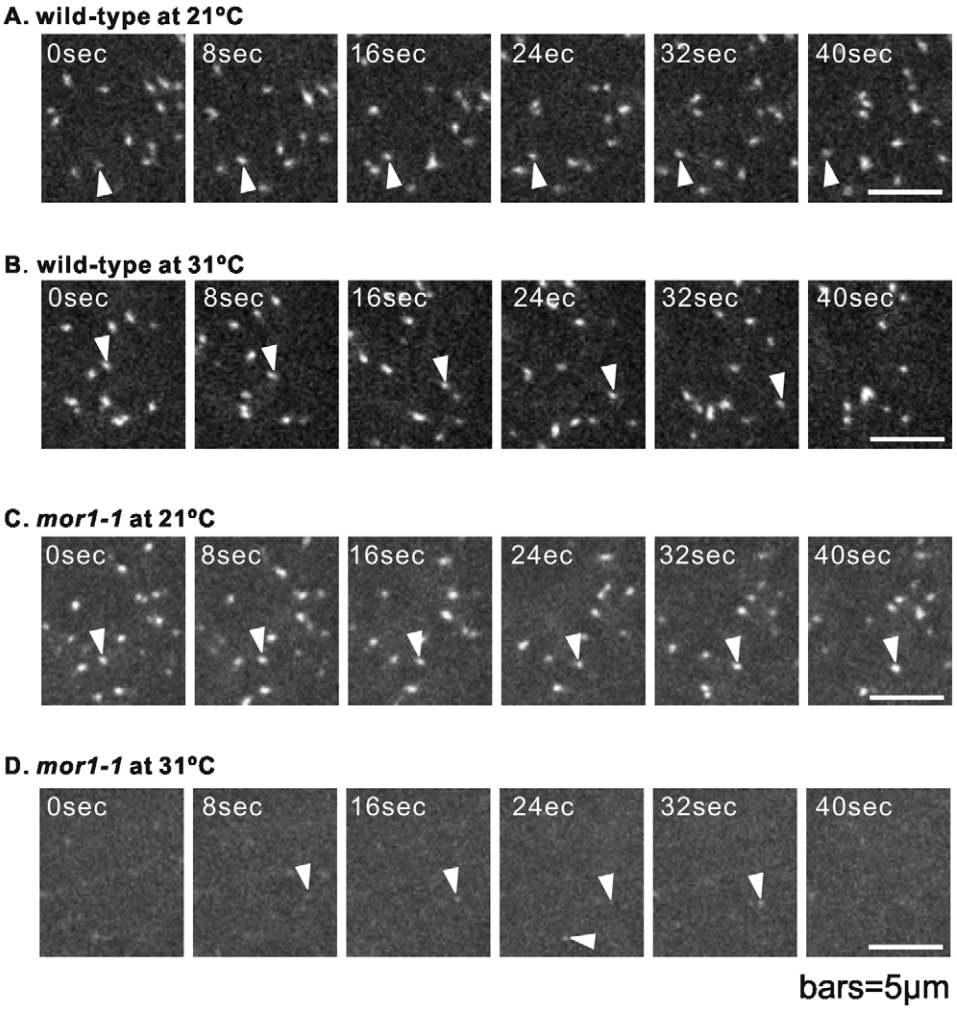


**Fig. 5.** EB1 comet intensity fluctuates in *mor1-1* mutants at 21°C and is greatly reduced at 31°C. (A,B) Transgenic *ProEB1*::EB1-GFP line (in wild-type background) at 21°C (A) and 31°C (B). (C,D) *mor1-1* expressing *ProEB1*::EB1-GFP at 21°C (C) and 31°C (D). Time-lapse images of *ProEB1*::EB1-GFP were collected as described in Fig. 4 but at 8 second intervals. To compare fluorescence between treatments, images were collected from the same cell with identical confocal settings before and after the temperature increase. The same contrast adjustments were applied to the images obtained from wild type and *mor1-1*. Arrowheads follow one comet between time frames in each series. Comets in *mor1-1* at 31°C (D) were less abundant and rarely persisted for several time frames (upper arrowheads) or were detected at only one time point (lower arrowhead) within a series. A-D correspond to Movies 5-8 in supplementary material. Bars, 5 μm.

function of MOR1. In Fig. 9, we present a putative interaction model in which one linear MOR1 protein associates with one tubulin protofilament within a microtubule polymer, with each of its five TOG domains spanning the bond between two adjacent tubulin dimers. We suggest that the N-terminal TOG domain (TOG1A) is situated at the plus end of the protofilament where it can recruit one free tubulin dimer at a time via the α-tubulin subunit, to promote polymer formation. This provides a mechanism for bringing free tubulin subunits into contact with the microtubule polymer in the correct orientation. According to our model, the successful addition of a new tubulin dimer promotes the partial dissociation of MOR1 from the protofilament so that it can move processively to repeat its polymerase activity. We propose that the remaining four TOG domains also have binding affinity for α- and β-tubulins but with strong preference for polymerized tubulin dimers. This mechanism will ensure the correct placement of MOR1 along the protofilament and, by working in the reverse direction when conditions favour disassembly, will assist in the rapid removal of tubulin subunits.

Our model integrates data from the current as well as several recent studies. First, XMAP215 family proteins that carry five TOG domains are predicted to be long and flexible proteins ~60 nm in length (Cassimeris et al., 2001) with each TOG domain 5.4-6.0 nm in length (Al-Bassam et al., 2007; Slep and Vale, 2007). Taking into account the inter-TOG regions, it is possible that TOG domains are spaced 8 nm apart, coinciding with the distance between tubulin dimers. Second, the suppression in yeast of β-tubulin mutations by amino acid substitutions in the fifth HEAT-like repeat of the TOG2 of the yeast Stu2 protein suggests that the C-terminal end of each TOG domain has a critical β-tubulin binding site (Wang and Huffaker, 1997). It is notable that both the *mor1-1* and *mor1-2* point mutations, which generate temperature-dependent microtubule disruption, occur in the fifth HEAT-like repeat of the first TOG domain. Third, it has been shown that the first TOG domain of Stu2, equivalent to TOG1A, can bind single free tubulin dimers but that the second TOG domain on its own does not (Al-Bassam et al., 2006). Fourth, high resolution tracking of individual XMAP215-GFP molecules in vitro suggests that they move with the growing or shrinking plus end (Brouhard et al., 2008), a form of movement akin to surfing (Asbury, 2008). Finally, size exclusion chromatography suggests a 1:1 tubulin:XMAP215 binding ratio (Brouhard et al., 2008).

The surfing model proposed by Brouhard et al. (Brouhard et al., 2008) differs from our model in predicting that the first two TOG domains work with the third and fourth TOG domains to trap just one tubulin dimer. Their model is supported by the appearance of negatively stained XMAP215:tubulin complexes assembled in vitro (Brouhard et al., 2008). The previously published templating model in which XMAP215 is predicted to recruit multiple tubulin dimers simultaneously was inspired by the in vitro ability of XMAP215 to speed up growth and shrinkage rates of microtubules in 40-60

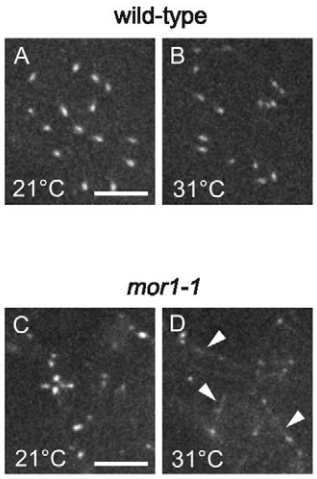


**Fig. 6.** EB1-GFP associates with microtubule side walls in *mor1-1* at 31°C. Changes in GFP-EB1 distribution patterns are shown for the same cells before and after the temperature increase using identical confocal settings and contrast adjustments. (A,B) Transgenic *ProEB1*::EB1-GFP in wild type at 21°C (A) and 31°C (B). Side wall labelling was not detected in wild type at 31°C. (C,D) *mor1-1* expressing *ProEB1*::EB1-GFP at 21°C (C) and 31°C (D). At 31°C, side wall labelling (arrowheads) became obvious in *mor1-1*. Bars, 5 μm.

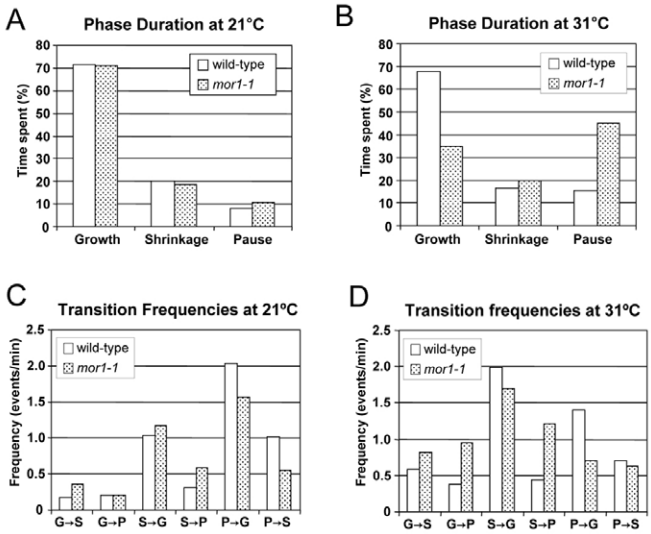


**Fig. 7.** Quantification of time spent in growth, shrinkage and pause, and transition frequencies between phases at 21°C and 31°C. (A,B) Relative duration of growth, shrinkage and pause events at 21°C (A) and 31°C (B). The sum of time every microtubule end spent in each phase was divided by the sum of time for which all microtubule plus ends were measured. (C,D) Transition frequencies between growth (G), shrinkage (S) and pause (P) at 21°C (C) and 31°C (D) were calculated by dividing the total number of transitions from one state to another by the total time spent in the initial state. Data were collected from 115 microtubules from six cells from four different plants for wild type at 21°C, 28 microtubules from seven cells from four different plants for wild type at 31°C, 98 microtubules from 5 cells from three different plants for *mor1-1* at 21°C, and 26 microtubules from 12 cells from nine different plants for *mor1-1* at 31°C. Epidermal cells from the abaxial surface of the first leaves from 11- to 12-day-old seedlings were used. Data were obtained from time-lapse images of microtubules expressing GFP-TUB in both wild type and *mor1-1* (as described in Fig. 1).

nm increments, which is equivalent to 4-7.5 tubulin dimers (Kerssemakers et al., 2006). The templating model is, thus, incompatible with the strict in vitro binding of one free tubulin dimer at a time for XMAP215 (Brouhard et al., 2008). By suggesting that only the N-terminal TOG domain recruits free tubulin, while the remaining four TOG domains can interact with already polymerized tubulins, our model attempts to resolve the differences between surfing and templating. Interestingly, the tobacco homologue of MOR1, TMBP200, has been shown to bind to tubulin oligomers in vitro (Hamada et al., 2004), suggesting that each TOG domain still retains the capacity to bind tubulin and that under certain conditions, oligomer association is feasible.

### MOR1 as an anti-pause factor

MOR1 appears to play a major role in suppressing the state known as microtubule pause. This may be a general attribute of MOR1 homologues. In vitro experiments have shown that full-length XMAP215 as well as N-terminal fragments destabilize microtubules that had first been stabilized in the paused state by treatment with the slowly hydrolysable GTP analogue GMPCPP (Shirasu-Hiza et al., 2003). RNAi-based depletion of MSPS in cultured *Drosophila melanogaster* interphase cells increases the time microtubules spend in pause (Brittle and Ohkura, 2005).

The function of MOR1 as an anti-pause factor may also be one of its most critical in terms of organizing the acentrosomal microtubule array found in the plant cell cortex. In *mor1-1* at permissive temperature, cortical arrays are well organized, with no apparent defects in spatial organization. This is somewhat surprising, given that we found that at 21°C microtubules in *mor1-1* grew and shrank more slowly than in wild type. By contrast, the proportions of time spent in growth, shrinkage and pause in *mor1-1* at 21°C were similar to those recorded for wild type. Therefore, microtubule pause events may be of greater detriment to the spatial organization of cortical microtubule arrays than low polymerization dynamics. This conclusion is supported by a recent report showing that changes in spatial organization of cortical microtubules in the *spiral2* mutant of *Arabidopsis* can be attributed solely to a modest change in the time spent in pause (Yao et al., 2008).

### Does MOR1 interact with EB1?

The plus end tracking protein EB1 is also likely to be involved in regulating the incidence of pause events, consistent with recent in vitro experiments showing that EB1 can promote the incidence of both catastrophe and rescue (Vitre et al., 2008). Although we used fluorescently tagged EB1b primarily as a means to measure plus end dynamics, we observed striking changes in EB1 labelling patterns in *mor1-1* mutants, suggesting that MOR1 modulates the association of EB1 with microtubules. Whether this is via direct interactions, as has been documented for EB1 and the MOR1 homologues Stu2 (Chen et al., 1998), DdCP224 (Rehberg and Graf, 2002) and XMAP215 (Niethammer et al., 2007) will require further analysis.

At the restrictive temperature, EB1 comets in *mor1-1* were unstable and relatively small. By contrast, microtubule side wall labelling by EB1 increased. The simplest explanation is that loss of high affinity EB1-binding at microtubule plus ends allows excess EB1 to bind to low affinity sites on the microtubule side walls. Alternatively, the mutant mor1-1 protein, which continues to be distributed along the full length of microtubules at the restrictive temperature (Kawamura et al., 2006), could either lose its normal ability to restrict EB1 to the growing plus end or switch its conformation so that it has increased affinity for EB1. With regard

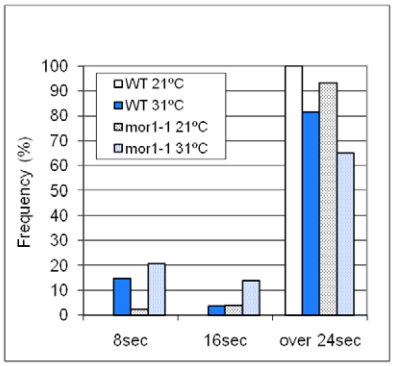


**Fig. 8.** MOR1 promotes the constant growth of microtubules. Distribution frequencies of the durations for one constant growth event were calculated from time-lapse images of GFP-TUB-labelled microtubules in wild type (WT) and *mor1-1* at 21°C and 31°C. Growth events were categorized as lasting at least 8 seconds (8 sec), at least 16 seconds (16 sec) or for more than 24 seconds. Constant growth was inhibited in *mor1-1* at 31°C. Data were collected from 115 microtubules from six cells from four different plants for wild type at 21°C, 28 microtubules from seven cells from four different plants for wild type at 31°C, 98 microtubules from five cells from three different plants for *mor1-1* at 21°C, and 26 microtubules from 12 cells from nine different plants for *mor1-1* 31°C.

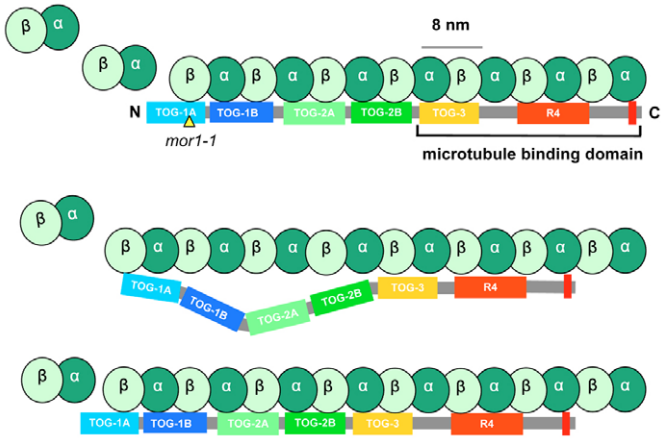


**Fig. 9.** A model for the interaction of MOR1 with microtubules and free tubulin. The predicted domain structure of MOR1 includes five N-terminal TOG domains and conserved C-terminal domains (red bars). The predicted 60 nm length of MOR1 (Cassimeris et al., 2001) and the 5.4-6.0 nm of each TOG domain (Al-Bassam et al., 2007; Slep and Vale, 2007) suggest that each TOG domain may be spaced one tubulin dimer apart along the microtubule. For simplicity, only one tubulin protofilament is shown. In vitro studies suggest that the C-terminal region (indicated with bracket) confers microtubule polymer binding (Twell et al., 2002). The location of the *mor1-1* point mutation, which substitutes a single amino acid in the first TOG domain, is indicated (yellow triangle). According to the data presented in our current study, this mutation site is critical for maintaining microtubule dynamics. Moreover, suppressor mutagenesis data from yeast suggests that this region interacts directly with β-tubulin (Wang and Huffaker, 1997). The model shown here suggests that MOR1 facilitates the docking of a free tubulin dimer via its first TOG domain (TOG1A), and then stabilizes the polymerization event by moving processively. The high affinity of TOG1A for free tubulin may stimulate a partial dissociation that is propagated along all the TOG domains in an inch worm-like manner to enable movement toward the microtubule plus end.

to this latter possibility, it has been demonstrated that XMAP215 isolated from metaphase extracts has high affinity for EB1 but that this physical interaction is lost during interphase (Niethammer et al., 2007). A recent study indicates that EB1 binds to microtubule side walls to help seam closure and that it remains bound to the seam for long periods (Sandblad et al., 2006). The extent of microtubule side wall labelling observed in *mor1-1* microtubules, however, is probably much greater than expected for seam binding alone.

EB1 is thought to associate with structures or chemicals found specifically at the growing microtubule plus ends (Tirnauer et al., 2002). It is possible that the changes in EB1 comet size and fluorescence intensity in *mor1-1* are caused by the GTP cap becoming unstable and smaller than normal. Indeed, it has been demonstrated that modifications to α-tubulin expected to inhibit the putative GTPase-activating domains of α-tubulin can increase the length of GFP-EB1 comets in *Arabidopsis* (Abe and Hashimoto, 2005). In the current study, however, we found that in wild-type cells at 31°C, EB1 comets moved more quickly but showed similar or weaker fluorescence intensity than at 21°C, suggesting either that GTP caps are not longer in faster growing microtubules or that there is no direct correlation between EB1 binding, GTP capping and growth rate. Furthermore, we found comet labelling in *mor1-1* to be reduced compared with that in wild type at both the permissive and restrictive temperatures, suggesting that the loss of *mor1-1* function rather than the velocity of microtubule growth is responsible for the reduced EB1 association. Clearly there are no simple relationships between comet velocity, labelling intensity and comet size.

Finally, we note for wild-type cells that microtubule plus end growth rates measured by EB1b-GFP comets were faster (4.9 μm/minute at 21°C and 8.2 μm/minute at 31°C) than those measured with the GFP-TUB reporter (3.5 μm/minute at 21°C and 6.5 μm/minute at 31°C). This increased polymerization rate could be caused by the expression of an extra copy of EB1b in these cells. By contrast, the presence of EB1b-GFP in the *mor1-1* mutant did not increase plus end growth rates and, in fact, the velocities measured with EB1b-GFP in *mor1-1* cells (2.3 μm/minute at 21°C and 1.4 μm/minute at 31°C) were slightly lower than those measured with the GFP-TUB reporter (2.5 μm/minute at 21°C and 2.0 μm/minute at 31°C). The inability of EB1b to increase microtubule plus end growth rates in the *mor1-1* mutant further supports the idea that MOR1 normally modulates the activity of EB1.

### Implications of temperature-dependent microtubule dynamics

In this study, we documented increases in microtubule dynamics in wild-type cells as temperatures were raised within a 10°C range (21 to 31°C) in which optimal growth and development will happen. The changes, observed using several different reporter proteins, were detected as early as 7 minutes after the temperature in the specimen chamber reached 31°C. That microtubules polymerize faster at higher temperatures is well known from in vitro studies, but relatively few studies have addressed how microtubule dynamics change in vivo in relation to higher temperatures. Previous studies in plants have documented changes in microtubule organization, but not dynamics, under heat stress conditions that are well above the temperatures used in our study. In one recent study using *Arabidopsis* roots, no obvious changes in cortical microtubule organization were observed at 34°C but cortical microtubule arrays became disrupted at 40-42°C (Muller et al., 2007). In tobacco VBI-0 suspension culture cells, cortical microtubule organization was altered at 38°C and became severely disrupted at 42°C (Smertenko et al., 1997).

The temperature-dependent alterations in microtubule dynamics in wild-type cells also should be considered when appraising phenotypes of other temperature-sensitive mutants. Like the *mor1* mutants, the *radially swelling* (*rsw*) mutants are temperature-sensitive and roots lose the ability to elongate properly at a restrictive temperatures of around 30°C (Baskin et al., 1992). Some mutants in this collection, such as *rsw6* (Bannigan et al., 2006) and *rsw7* (Bannigan et al., 2007), have disorganized microtubule arrays at the restrictive temperature, and the radial swelling phenotypes may result in the inability of microtubule dynamics to increase at higher temperatures. Other mutants, such as *rsw1* (Arioli et al., 1998; Sugimoto et al., 2001) and *rsw2* (*korr*) (Lane et al., 2001) are defective in cellulose microfibril synthesis, a process that is linked both spatially and functionally to cortical microtubules (Wasteneys, 2004). Altered microtubule dynamics might help adjust the mechanical properties of cellulose microfibrils as growth rates change in a temperature-dependent manner. Thus, failure of the cellulose synthesis machinery to adapt to increased microtubule dynamics and/or general metabolic stimulation at the high end of the normal temperature range could account for the conditional *rsw* phenotypes.

Measurements of cortical microtubule dynamics in plant cells so far indicate some variations in microtubule dynamic parameters that may in part be attributed to species and cell type (Vos et al., 2004). It remains possible that these reported variations could be caused by variations in ambient temperatures in different laboratories. Our results highlight the need to carefully monitor and to standardize culture temperatures during live cell imaging of plant cells.

## Materials and Methods

### Plant material and growth conditions

Seeds were planted on Petri plates containing Hoagland's medium as described previously (Himmelspach et al., 2003) with the exception that plates were stored at 4°C for 3-5 days before being transferred to a growth cabinet, and that plants were grown under constant light (80 μmol $m^{-2}$ $second^{-1}$) at 21°C for 11-12 days. The *Arabidopsis thaliana* ecotype Columbia *mor1-1* mutant (GenBank accession no. AF367246) (Whittington et al., 2001), was backcrossed eight times to the parental Columbia ecotype. Transgenic plants of GFP-TUA (Ueda et al., 1999), GFP-TUB (Nakamura et al., 2004) in the Columbia background (Abe and Hashimoto, 2005) and *ProEB1*::EB1b-GFP (Dixit et al., 2006) were crossed to the eight times backcrossed *mor1-1*. $F_3$ segregants homozygous for both *GFP* and *mor1-1* or wild-type *MOR1* were used in this study.

### Live cell imaging

The outermost halves of the first true leaves of 11- to 12-day-old seedlings were excised and placed on a coverslip that formed the bottom of a culture dish (Electron Microscopy Sciences, Hatfield, PA). Leaf cuttings were mounted in water with their abaxial side facing the coverslip and a piece of 2% agar was placed on top to stabilize the leaves. Culture dishes were kept at either 21°C or 31°C for at least 1 hour before observation. Samples were observed not more than 4.5 hours after leaves were excised. For image collection, a Quorum Wave FX Spinning Disc Confocal System (Quorum, Guelph, Ontario, Canada) with a 63× 1.3 NA glycerol-immersion lens or a Bio-Rad Radiance Plus confocal microscope (Carl Zeiss, Jena, Thuringia, Germany) with a 63× 1.4 NA oil-immersion lens was used. The Quorum Wave FX Spinning Disc Confocal System consisted of a Leica DMI6000B microscope (Leica, Wetzlar, Germany), a CSU10 Confocal Scan Unit (Yokogawa Electric Corporation, Tokyo, Japan), Electron Multiplier-CCD Digital Camera C9100-13 (Hamamatsu Photonics K. K., Hamamatsu, Shizuoka, Japan) and a MS2000 Piezo Z Stage (Applied Scientific Instrumentation, Inc., Eugene, OR), and used the 491 nm line of a Cobolt Calypso continuous-wave diode-pumped solid-state laser (Cobolt AB, Stockholm, Sweden). For the Bio-Rad Radiance Plus confocal microscope, the 488 nm line of an Ar laser was used for GFP excitation. To record microtubule dynamics at the permissive or restrictive temperatures of *mor1-1*, a Bionomic Controller BC-110 together with a Heat Exchanger HEC-400, a Bionomic Controller BC-100 (20-20 Technology Inc, Wilmington, NC) temperature-controlled stage and an objective heater (Bioptechs, Butler, PS) were used. Desired temperatures in the culture dish with a piece of 2% agar right above an objective were ensured by a thermocouple FLUKE52 (John Fluke MFG. Co., Inc., Everett, WA). Upon temperature shifts, temperatures in the culture dish reached the newly set temperature after about 8 minutes. Images were taken every 8 seconds over 3-5 minutes for GFP-TUB and every 5 or 8 seconds over 40-60 seconds for *ProEB1*::EB1b-GFP.

### Image analysis

Images were processed with ImageJ (http://rsb.info.nih.gov/ij/) for contrast adjustment and creation of movies from time-lapse imaging, and with Corel Draw for resampling. Kymographs were created with ImageJ Multiple Kymograph (http://www.embl.de/eamnet/html/body_kymograph.html). Microtubule dynamics were measured with ImageJ Manual Tracking. Microtubule ends were not always clear, sometimes spanning few pixels with a diminishing signal, and the resolution limit of a confocal microscope is 0.2 μm. Therefore, changes in length of less than ±0.4 μm between two time points was considered pause, with the following exceptions. When an increment less than 0.4 μm was followed by growth or was observed over more than three successive measurements, it was considered to be growth. Shrinkage was determined in a similar manner. Transition frequencies were calculated by dividing the total number of one type of transition event by the total time spent for the original state (i.e. transition frequency from A to B was calculated by dividing the total number of transition events from A to B by the total time spent for A) (Howell et al., 1999; Walker et al., 1988). Microtubule ends that were followed for more than three time points were included in the transition frequency analysis. The frequency of time spent for one constant growth event was calculated by dividing the total number of one continuous growth event that lasted 8 seconds or 16 seconds or over 24 seconds by the total number of continuous growth events. When the beginning and/or ending of a growth event could not be determined because of imaging timing or a focus issue, growth events that lasted more than 24 seconds were included.

To compare the fluorescence intensity of EB1b-GFP comets, maximum intensities of all comets in a fixed area (40×50 pixels) were measured from images collected from the same cells before and after shifting the temperature from 21°C to 31°C. Because the expression levels differed among cells, the changes in ratio rather than actual pixel intensities were compared. The Wilcoxon signed-rank test was used to compare the changes in each cell. A total of at least 54 comets were examined in all cases. The sample numbers were nine cells from three plants for wild type and nine cells from five plants for *mor1-1*.

We thank Takashi Hashimoto (NAIST, Japan) for the *35S::GFP-TUB* and *35S::GFP-TUA* lines, and Richard Cyr (Penn State University, PA) for the *ProEB1::EB1b-GFP* line. We thank Kevin Hodgson (UBC Bioimaging Facility) for assistance with microscopy and Madeleine Rashbrooke (Australian National University) for MOR1 structural domain analysis. This work was supported by a Canadian Institutes of Health Research, Research Resource Grant (PRG-80159), a Canadian Institutes of Health Research Operating Grant (MOP-86675) and a Natural Sciences and Engineering Research Council Discovery Grant to G.O.W., and a UBC University Graduate Fellowship to E.K.

## References

**Abe, T. and Hashimoto, T.** (2005). Altered microtubule dynamics by expression of modified alpha-tubulin protein causes right-handed helical growth in transgenic Arabidopsis plants. *Plant J.* **43**, 191-204.

**Al-Bassam, J., van Breugel, M., Harrison, S. C. and Hyman, A.** (2006). Stu2p binds tubulin and undergoes an open-to-closed conformational change. *J. Cell Biol.* **172**, 1009-1022.

**Al-Bassam, J., Larsen, N. A., Hyman, A. A. and Harrison, S. C.** (2007). Crystal structure of a TOG domain: conserved features of XMAP215/Dis1-family TOG domains and implications for tubulin binding. *Structure* **15**, 355-362.

**Arioli, T., Peng, L., Betzner, A. S., Burn, J., Wittke, W., Herth, W., Camilleri, C., Hofte, H., Plazinski, J., Birch, R. et al.** (1998). Molecular analysis of cellulose biosynthesis in Arabidopsis. *Science* **279**, 717-720.

**Asbury, C. L.** (2008). XMAP215: a tip tracker that really moves. *Cell* **132**, 19-20.

**Bannigan, A., Wiedemeier, A. M., Williamson, R. E., Overall, R. L. and Baskin, T. I.** (2006). Cortical microtubule arrays lose uniform alignment between cells and are oryzalin resistant in the Arabidopsis mutant, radially swollen 6. *Plant Cell Physiol.* **47**, 949-958.

**Bannigan, A., Scheible, W. R., Lukowitz, W., Fagerstrom, C., Wadsworth, P., Somerville, C. and Baskin, T. I.** (2007). A conserved role for kinesin-5 in plant mitosis. *J. Cell Sci.* **120**, 2819-2827.

**Baskin, T. I., Betzner, A. S., Hoggart, R., Cork, A. and Williamson, R. E.** (1992). Root morphology mutants in Arabidopsis thaliana. *Aust. J. Plant Physiol.* **19**, 427-437.

**Bisgrove, S. R., Hable, W. E. and Kropf, D. L.** (2004). +TIPs and microtubule regulation. The beginning of the plus end in plants. *Plant Physiol.* **136**, 3855-3863.

**Brittle, A. L. and Ohkura, H.** (2005). Mini spindles, the XMAP215 homologue, suppresses pausing of interphase microtubules in Drosophila. *EMBO J.* **24**, 1387-1396.

**Brouhard, G. J., Stear, J. H., Noetzel, T. L., Al-Bassam, J., Kinoshita, K., Harrison, S. C., Howard, J. and Hyman, A. A.** (2008). XMAP215 is a processive microtubule polymerase. *Cell* **132**, 79-88.

**Cassimeris, L. and Morabito, J.** (2004). TOGp, the human homolog of XMAP215/Dis1, is required for centrosome integrity, spindle pole organization, and bipolar spindle assembly. *Mol. Biol. Cell* **15**, 1580-1590.

**Cassimeris, L., Gard, D., Tran, P. T. and Erickson, H. P.** (2001). XMAP215 is a long thin molecule that does not increase microtubule stiffness. *J. Cell Sci.* **114**, 3025-3033.
**Chen, X. P., Yin, H. and Huffaker, T. C.** (1998). The yeast spindle pole body component Spc72p interacts with Stu2p and is required for proper microtubule assembly. *J. Cell Biol.* **141**, 1169-1179.
**Collings, D. A., Lill, A. W., Himmelspach, R. and Wasteneys, G. O.** (2006). Hypersensitivity to cytoskeletal antagonists demonstrates microtubule-microfilament cross-talk in the control of root elongation in Arabidopsis thaliana. *New Phytol.* **170**, 275-290.
**Dixit, R., Chang, E. and Cyr, R.** (2006). Establishment of polarity during organization of the acentrosomal plant cortical microtubule array. *Mol. Biol. Cell* **17**, 1298-1305.
**Gard, D. L. and Kirchner, M. W.** (1987). A microtubule-associated protein from Xenopus eggs that specifically promotes assembly at the plus-end. *J. Cell Biol.* **105**, 2203-2215.
**Gard, D. L., Becker, B. E. and Josh Romney, S.** (2004). MAPping the eukaryotic tree of life: structure, function, and evolution of the MAP215/Dis1 family of microtubule-associated proteins. *Int. Rev. Cytol.* **239**, 179-272.
**Hamada, T., Igarashi, H., Itoh, T. J., Shimmen, T. and Sonobe, S.** (2004). Characterization of a 200 kDa microtubule-associated protein of tobacco BY-2 cells, a member of the XMAP215/MOR1 family. *Plant Cell Physiol.* **45**, 1233-1242.
**Himmelspach, R., Williamson, R. E. and Wasteneys, G. O.** (2003). Cellulose microfibril alignment recovers from DCB-induced disruption despite microtubule disorganization. *Plant J.* **36**, 565-575.
**Howell, B., Larsson, N., Gullberg, M. and Cassimeris, L.** (1999). Dissociation of the tubulin-sequestering and microtubule catastrophe-promoting activities of oncoprotein 18/stathmin. *Mol. Biol. Cell* **10**, 105-118.
**Kawamura, E., Himmelspach, R., Rashbrooke, M. C., Whittington, A. T., Gale, K. R., Collings, D. A. and Wasteneys, G. O.** (2006). MICROTUBULE ORGANIZATION 1 regulates structure and function of microtubule arrays during mitosis and cytokinesis in the Arabidopsis root. *Plant Physiol.* **140**, 102-114.
**Kerssemakers, J. W., Munteanu, E. L., Laan, L., Noetzel, T. L., Janson, M. E. and Dogterom, M.** (2006). Assembly dynamics of microtubules at molecular resolution. *Nature* **442**, 709-712.
**Kinoshita, K., Arnal, I., Desai, A., Drechsel, D. N. and Hyman, A. A.** (2001). Reconstitution of physiological microtubule dynamics using purified components. *Science* **294**, 1340-1343.
**Konishi, M. and Sugiyama, M.** (2003). Genetic analysis of adventitious root formation with a novel series of temperature-sensitive mutants of *Arabidopsis thaliana*. *Development* **130**, 5637-5647.
**Kosco, K. A., Pearson, C. G., Maddox, P. S., Wang, P. J., Adams, I. R., Salmon, E. D., Bloom, K. and Huffaker, T. C.** (2001). Control of microtubule dynamics by Stu2p is essential for spindle orientation and metaphase chromosome alignment in yeast. *Mol. Biol. Cell* **12**, 2870-2880.
**Lane, D. R., Wiedemeier, A., Peng, L., Hofte, H., Vernhettes, S., Desprez, T., Hocart, C. H., Birch, R. J., Baskin, T. I., Burn, J. E. et al.** (2001). Temperature-sensitive alleles of RSW2 link the KORRIGAN endo-1,4-beta-glucanase to cellulose synthesis and cytokinesis in Arabidopsis. *Plant Physiol.* **126**, 278-288.
**Marc, J., Granger, C. L., Brincat, J., Fisher, D. D., Kao, T., McCubbin, A. G. and Cyr, R. J.** (1998). A GFP-MAP4 reporter gene for visualizing cortical microtubule rearrangements in living epidermal cells. *Plant Cell* **10**, 1927-1940.
**Muller, J., Menzel, D. and Samaj, J.** (2007). Cell-type-specific disruption and recovery of the cytoskeleton in Arabidopsis thaliana epidermal root cells upon heat shock stress. *Protoplasma* **230**, 231-242.
**Nakamura, M., Naoi, K., Shoji, T. and Hashimoto, T.** (2004). Low concentrations of propyzamide and oryzalin alter microtubule dynamics in Arabidopsis epidermal cells. *Plant Cell Physiol.* **45**, 1330-1334.
**Niethammer, P., Kronja, I., Kandels-Lewis, S., Rybina, S., Bastiaens, P. and Karsenti, E.** (2007). Discrete states of a protein interaction network govern interphase and mitotic microtubule dynamics. *PLoS Biol.* **5**, e29.
**Popov, A. V. and Karsenti, E.** (2003). Stu2p and XMAP215: turncoat microtubule-associated proteins? *Trends Cell Biol.* **13**, 547-550.
**Rehberg, M. and Graf, R.** (2002). Dictyostelium EB1 is a genuine centrosomal component required for proper spindle formation. *Mol. Biol. Cell* **13**, 2301-2310.
**Sandblad, L., Busch, K. E., Tittmann, P., Gross, H., Brunner, D. and Hoenger, A.** (2006). The Schizosaccharomyces pombe EB1 homolog Mal3p binds and stabilizes the microtubule lattice seam. *Cell* **127**, 1415-1424.
**Shirasu-Hiza, M., Coughlin, P. and Mitchison, T.** (2003). Identification of XMAP215 as a microtubule-destabilizing factor in Xenopus egg extract by biochemical purification. *J. Cell Biol.* **161**, 349-358.
**Slep, K. C. and Vale, R. D.** (2007). Structural basis of microtubule plus end tracking by XMAP215, CLIP-170, and EB1. *Mol. Cell* **27**, 976-991.
**Smertenko, A., Draber, P., Viklicky, V. and Opatrny, Z.** (1997). Heat stress affects the organization of microtubules and cell division in Nicotiana tabacum cells. *Plant Cell Environ.* **20**, 1534-1542.
**Sugimoto, K., Williamson, R. E. and Wasteneys, G. O.** (2001). Wall architecture in the cellulose-deficient rsw1 mutant of Arabidopsis thaliana: microfibrils but not microtubules lose their transverse alignment before microfibrils become unrecognizable in the mitotic and elongation zones of roots. *Protoplasma* **215**, 172-183.
**Sugimoto, K., Himmelspach, R., Williamson, R. E. and Wasteneys, G. O.** (2003). Mutation or drug-dependent microtubule disruption causes radial swelling without altering parallel cellulose microfibril deposition in Arabidopsis root cells. *Plant Cell* **15**, 1414-1429.
**Tirnauer, J. S., Grego, S., Salmon, E. D. and Mitchison, T. J.** (2002). EB1-microtubule interactions in Xenopus egg extracts: role of EB1 in microtubule stabilization and mechanisms of targeting to microtubules. *Mol. Biol. Cell* **13**, 3614-3626.
**Tournebize, R., Popov, A., Kinoshita, K., Ashford, A. J., Rybina, S., Pozniakovsky, A., Mayer, T. U., Walczak, C. E., Karsenti, E. and Hyman, A. A.** (2000). Control of microtubule dynamics by the antagonistic activities of XMAP215 and XKCM1 in Xenopus egg extracts. *Nat. Cell Biol.* **2**, 13-19.
**Twell, D., Park, S. K., Hawkins, T. J., Schubert, D., Schmidt, R., Smertenko, A. and Hussey, P. J.** (2002). MOR1/GEM1 has an essential role in the plant-specific cytokinetic phragmoplast. *Nat. Cell Biol.* **4**, 711-714.
**Ueda, K., Matsuyama, T. and Hashimoto, T.** (1999). Visualization of microtubules in living cells of transgenic Arabidopsis thaliana. *Protoplasma* **206**, 201-206.
**van Breugel, M., Drechsel, D. and Hyman, A.** (2003). Stu2p, the budding yeast member of the conserved Dis1/XMAP215 family of microtubule-associated proteins is a plus end-binding microtubule destabilizer. *J. Cell Biol.* **161**, 359-369.
**Vasquez, R. J., Gard, D. L. and Cassimeris, L.** (1994). XMAP from Xenopus eggs promotes rapid plus end assembly of microtubules and rapid microtubule polymer turnover. *J. Cell Biol.* **127**, 985-993.
**Vasquez, R. J., Gard, D. L. and Cassimeris, L.** (1999). Phosphorylation by CDK1 regulates XMAP215 function *in vitro*. *Cell Motil. Cytoskeleton* **43**, 310-321.
**Vitre, B., Coquelle, F. M., Heichette, C., Garnier, C., Chretien, D. and Arnal, I.** (2008). EB1 regulates microtubule dynamics and tubulin sheet closure *in vitro*. *Nat. Cell Biol.* **10**, 415-421.
**Vos, J. W., Dogterom, M. and Emons, A. M.** (2004). Microtubules become more dynamic but not shorter during preprophase band formation: a possible "search-and-capture" mechanism for microtubule translocation. *Cell Motil. Cytoskeleton* **57**, 246-258.
**Walker, R. A., O'Brien, E. T., Pryer, N. K., Soboeiro, M. F., Voter, W. A., Erickson, H. P. and Salmon, E. D.** (1988). Dynamic instability of individual microtubules analyzed by video light microscopy: rate constants and transition frequencies. *J. Cell Biol.* **107**, 1437-1448.
**Wang, P. J. and Huffaker, T. C.** (1997). Stu2p: A microtubule-binding protein that is an essential component of the yeast spindle pole body. *J. Cell Biol.* **139**, 1271-1280.
**Wasteneys, G. O.** (2004). Progress in understanding the role of microtubules in plant cells. *Curr. Opin. Plant Biol.* **7**, 651-660.
**Wasteneys, G. O. and Yang, Z.** (2004). New views on the plant cytoskeleton. *Plant Physiol.* **136**, 3884-3891.
**Whittington, A. T., Vugrek, O., Wei, K. J., Hasenbein, N. G., Sugimoto, K., Rashbrooke, M. C. and Wasteneys, G. O.** (2001). MOR1 is essential for organizing cortical microtubules in plants. *Nature* **411**, 610-613.
**Yao, M., Wakamatsu, Y., Itoh, T. J., Shoji, T. and Hashimoto, T.** (2008). *Arabidopsis* SPIRAL2 promotes uninterrupted microtubule growth by suppressing the pause state of microtubule dynamics. *J. Cell Sci.* **121**, 2372-2381.

Journal of Cell Science